Advances in Nano Research, *Vol. 13, No.5 (2022) 453-463*
https://doi.org/10.12989/anr.2022.13.5.453

Free vibration analysis of FGP nanobeams with classical and non-classical boundary conditions using State-space approach

Youcef Tlidji[1], Rabia Benferhat[1,2], Tahar Hassaine Daouadji*[1,2], Abdelouahed Tounsi[4,5,6] and L.Cong Trinh[3]

[1]*Department of Civil Engineering, University of Tiaret, Algeria*
[2]*Laboratory of Geomatics and Sustainable Development, University of Tiaret, Algeria*
[3]*Faculty of Civil Engineering and Applied Mechanics, University of Technical Education Ho Chi Minh City, Viet Nam*
[4]*YFL (Yonsei Frontier Lab), Yonsei University, Seoul, Korea*
[5]*Department of Civil and Environmental Engineering, King Fahd University of Petroleum & Minerals, 31261 Dhahran, Eastern Province, Saudi Arabia*
[6]*Material and Hydrology Laboratory, University of Sidi Bel Abbes, Civil Engineering Department, Algeria*

(*Received October 3, 2021, Revised April 30, 2022, Accepted May 1, 2022*)

Abstract. This paper aims to investigate the vibration analysis of functionally graded porous (FGP) beams using State-space approach with several classical and non-classical boundary conditions. The materials properties of the porous FG beams are considered to have even and uneven distributions profiles along the thickness direction. The equation of motion for FGP beams with various boundary conditions is obtained through Hamilton's principle. State-space approach is used to obtain the governing equation of porous FG beam. The comparison of the results of this study with those in the literature validates the present analysis. The effects of span-to-depth ratio (L/h), of distribution shape of porosity and others parameters on the dynamic behavior of the beams are described. The results show that the boundary conditions, the geometry of the beams and the distribution shape of porosity affect the fundamental frequencies of the beams.
Keywords: FGP nanobeams; several boundary conditions; state-space approach; vibration analysis

1. Introduction

Composite beams have found increasing applications in a variety of engineering fields such as aerospace, civil, and marine during the recent decades. It becomes an obvious trend that more and more this type of beams will be used in the design of structural components. However, the use of the composite materials was limited by the high temperature until the appearance of new material known as functionally graded material (FGM). Due to its inherent smooth and continuous variation of material properties along some preferred direction, many scientists are attracted by the FGM. Many researchers have studied the vibration problems of FGMs beams. Wattanasakulpong and Ungbhakorn (2014) studied the free vibration of FG Euler-Bernoulli beams using the differential transformation method. The power law distribution of the materials was used to describe the material properties of FG beams. Wattanasakulpong and Ungbhakorn (2012) studied the linear and non-linear vibration of FGM Euler-Bernoulli beams having porosities with elastically restrained ends using the differential transformation method. The modified rule of mixture was used to describe the material properties of the FG beams with porosity. It was found that increasing the volume fraction of porosity leads to a decrease in natural frequency and an increase in non-linear natural frequency ratios (Xinli Xu *et al.* 2021, Ran Bi *et al.* 2021, Akhavan*et al.* 2021, Singh *et al.* 2021, Nazemnezhad *et al.* 2021, Ebrahimi *et al.* 2021, Bian*et al.* 2022, Ebrahimi *et al.* 2020). The fundamental frequency of FG beams with different boundary conditions was studied by Simsek (2009) using different higher-order beam theories. It was concluded that the fundamental frequencies increase as the slenderness ratio increases and decrease as the value of the power law exponent increases. Recently, Benferhat *et al.* (2021) presented vibrations analysis of simply supported rectangular FGM plate, a new hyperbolic shear deformation theory was introduced in their model in order to derive the governing equations by applying Hamilton's principle. Kablia *et al.* (2020) developed exact closed-form solutions for dynamic analysis of rectangular FGM plates with different boundary conditions they investigated the influence of the volume fraction and Geometry on the free vibration characteristics of FGM plates. Tlidji *et al.* (2021a) used modified differential method based on Euler–Bernoulli beam theory to solve governing differential equations of FGM beams (She *et al.* 2020, She 2020, Civalek *et al.* 2020, Hassaine Daouadji *et al.* 2021a, c, Rabahi *et al.* 2021d, Sayyid *et al.* 2020, Benferhat *et al.* 2018, 2021b, Adim *et al.* 2016b, Benhenni *et al.* 2018, Bensattalah *et al.* 2018, Rabahi *et al.* 2021b, Bensattalah *et al.* 2019, Ammar *et al.* 2020 and Farzad *et al.* 2020). Aydogdu and Taskin (2007) analysed free vibrations of simply supported FGM beams with comparative study between the classical beam

*Corresponding author, Professor, Ph.D.,
E-mail: daouadjitahar@gmail.com;
tahar.daouadji@univ-tiaret.dz

ISSN: 2287-237X (Print), 2287-2388 (Online)

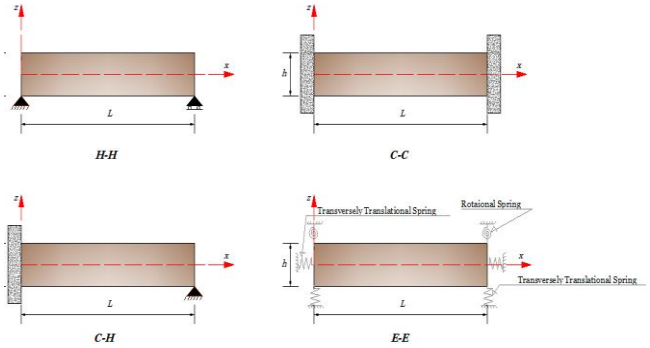

Fig. 1 FGP beams with classical and non-classical boundary conditions

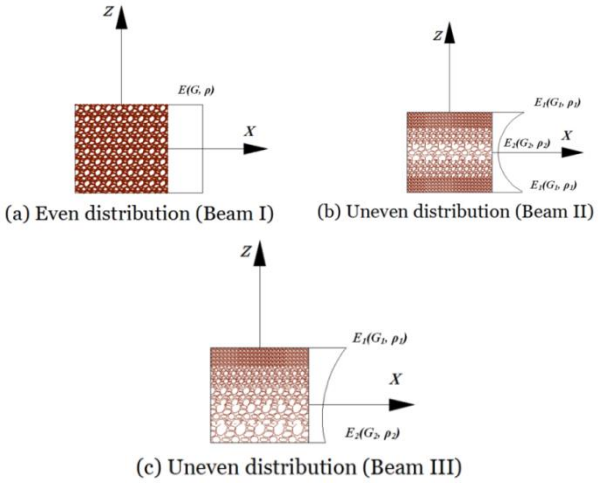

Fig. 2 Distributions of porosity in cross-sections of beams

theory (CBT), higher-order shear deformation theory (Reddy 1984, Hassaine Daouadji *et al*. 2021e, Rabahi *et al*. 2021e, Benferhat*et al*. 2021c, Karama *et al*. 2003). It is observed from the literature that there are many interesting approaches to analyze the behavior of classical anisotropic beams (Avcar Mehmet 2019, Benferhat *et al*. 2021, Rabahi *et al*. 2021a, f, Hassaine Daouadji *et al*. 2021d, Tounsi *et al*. 2020, Mohsen *et al*. 2020, Adim *et al*. 2016a, Mohammad *et al*. 2020, Reza *et al*. 2020, Noroozi *et al*. 2020, Dehshahri *et al*. 2020, Ersin *et al*. 2020, Yaser *et al*. 2020, Shanab *et al*. 2020, Ebrahimi *et al*. 2019, Benhenni *et al*. 2019, Bensattalah *et al*. 2020, Fakher *et al*. 2022, Mahsa *et al*. 2021, Bourada *et al*. 2019, Tlidji *et al*. 2021b, Abdelhak *et al*. 2021, Benferhat *et al*. 2019, 2021a, Bekki *et al*. 2019, 2021, Ben Henni *et al*. 2021, Chergui *et al*. 2019, Chaded *et al*. 2018, Hamrat *et al*. 2020, Hassaine Daouadji 2017, 2021b, Rabahi *et al*. 2021c, Bensatallah *et al*. 2021, Abdelhak *et al*. 2016, Abdedezak *et al*. 2018, Adim *et al*. 2018, Berghouti *et al*. 2019, Zaoui *et al*. 2017).

In the present study, the vibration analysis of functionally graded porous (FGP) beams using State-space approach with several classical and non-classical boundary conditions was investigated by using a new refined beam theory. The most interesting feature of this theory is that it accounts for a parabolic variation of the transverse shear strains across the thickness and satisfies the zero traction boundary conditions on the top and bottom surfaces of the beam without using shear correction factors. Then, the materials properties of the porous FG beams are considered to have even and uneven distributions profiles along the thickness direction. The equation of motion for FGP beams with various boundary conditions is obtained through Hamilton's principle. State-space approach is used to obtain the governing equation of porous FG beam. In this study, the effects of boundary conditions, volume fraction index, material properties, beam theory, slenderness ratio, and porosity on the natural frequencies are examined. Analytical solutions for vibration are obtained. Numerical examples are presented to verify the accuracy of the present theory. The results obtained in this paper are believed to be a reference for other researchers to compare with.

2. Theory and formulation:

2.1 Material properties:

This work considers a rectangular functionally graded porous (FGP) beam with length (L) in the x-axis and thickness (h) in the z-axis. The boundary conditions of the FGP beams are considered of classical and non-classical types (Fig. 1).

In the thickness direction of the beam, material parameters such as effective elastic modulus (E), shear modulus (G), and material density (ρ) vary according to three types of porosity distributions, as illustrated in Fig. 2.

The first is the Beam-I uniform porous distribution, in which the Young's modulus, shear modulus, and masse density are calculated as follows:

$$\begin{cases} E(z) = E_1(1 - e_0\eta) \\ G(z) = G_1(1 - e_0\eta) \\ \rho(z) = \rho_1(1 - e_m\eta) \end{cases} \quad (1a)$$

$$\eta = \frac{1}{e_0} - \frac{1}{e_0}\left(\frac{2}{\pi}\sqrt{1 - e_0} - \frac{2}{\pi} + 1\right)^2 \quad (1b)$$

Non-uniform porous distributions, designated as Beam II and Beam III, are the second and third, respectively. In this case, the material properties can be determined as follows:

for Beam-II:

$$\begin{cases} E(z) = E_1\left(1 - e_0\, coscos\left(\frac{\pi z}{h}\right)\right) \\ G(z) = G_1\left(1 - e_0\, coscos\left(\frac{\pi z}{h}\right)\right) \\ \rho(z) = \rho_1\left(1 - e_m\, coscos\left(\frac{\pi z}{h}\right)\right) \end{cases} \quad (2)$$

and for Beam-III:

$$\begin{cases} E(z) = E_1\left(1 - e_0\, coscos\left(\frac{\pi z}{2h} + \frac{\pi}{4}\right)\right) \\ G(z) = G_1\left(1 - e_0\, coscos\left(\frac{\pi z}{2h} + \frac{\pi}{4}\right)\right) \\ \rho(z) = \rho_1\left(1 - e_m\, coscos\left(\frac{\pi z}{2h} + \frac{\pi}{4}\right)\right) \end{cases} \quad (3)$$

where $e_0 = 1 - \frac{E_0}{E_1}$ is the porosity coefficient, and $e_m = 1 - \frac{\rho_0}{\rho_1}$ is the porosity coefficient for the mass density, respectively. The relationship between the porosity coefficients can be expressed as:

$$\frac{E_0}{E_1} = \left(\frac{\rho_0}{\rho_1}\right)^2 \rightarrow e_m = 1 - \sqrt{1 - e_0} \tag{4}$$

E_0 and E_1 are the minimum and maximum values of the modulus of elasticity, $G_1 = \frac{E_1}{2[1+\nu]}$ is the maximum value of shear modulus. The minimum and highest values of mass density are $\rho_0$and ρ_1. In this paper, the Poison's ratio (ν) is considered to be constant.

2.2 FGP beam vibration study using the Timoshenko beam theory

The displacements of an arbitrary point in a beam along the x and z axes, according to the Timoshenko beam theory, are$u(x,t)$and $w(x,t)$, respectively.

$$\begin{cases} u(x,t) = u_0(x,t) + z\phi(x,t) \\ w(x,t) = w_0(x,t) \end{cases} \tag{5}$$

In the mid-plane, $u_0(x,t)$ is the axial displacement and $w_0(x,t)$ is the transverse displacement. $\phi(x,t)$ is the rotational displacement of the beam cross-section and t is the time.

In Eq. (4), the strain associated with displacement can be calculated as:

$$\begin{cases} \varepsilon_{xx} = \dfrac{\partial u_0(x,t)}{\partial x} + z\dfrac{\partial \phi(x,t)}{\partial x} \\ \gamma_{xz} = \dfrac{\partial w_0(x,t)}{\partial x} + \phi \end{cases} \tag{6}$$

The stress field of the FGP beam can be formulated as follows using Hooke's law:

$$\begin{cases} \sigma_{xx} = \dfrac{E(z)}{(1-\nu^2)}\varepsilon_{xx} \\ \tau_{xz} = \dfrac{E(z)}{2(1+\nu)}\gamma_{xz} \end{cases} \tag{7}$$

where σ_{xx} and τ_{xz} denote the normal and shear stresses, respectively. The governing equations for FG porous beams can be derived using Hamilton's principle as follows:

$$\begin{cases} \dfrac{\partial N_x}{\partial x} = I_0\dfrac{\partial^2 u_0}{\partial t^2} + I_1\dfrac{\partial^2 \phi}{\partial t^2} \\ \dfrac{\partial Q_{xz}}{\partial x} = I_0\dfrac{\partial^2 w_0}{\partial t^2} \\ \dfrac{\partial M_x}{\partial x} - Q_{xz} = I_1\dfrac{\partial^2 u_0}{\partial t^2} + I_2\dfrac{\partial^2 \phi}{\partial t^2} \end{cases} \tag{8}$$

The following are characteristics of inertia:

$$(I_0, I_1, I_2) = \int_{-\frac{h}{2}}^{\frac{h}{2}} \rho(z)[1, z, z^2]bdz \tag{9}$$

The stress and moment outcomes are as follows:

$$\begin{cases} N_x = Au_0' - B\phi' \\ Q_{xz} = k_s A_{55}(w_0' + \phi) \\ M_x = Bu_0' - D\phi' \end{cases} \tag{10}$$

where $k_s = \frac{5}{6}$ is the shear correction factor; and the different stiffness parameters are characterized as follows:

$$[A, B, D] = \int_{-\frac{h}{2}}^{\frac{h}{2}} [1, z, z^2]\frac{E(z)}{(1-\nu^2)}bdz \tag{11}$$

$$A_{55} = \int_{-\frac{h}{2}}^{\frac{h}{2}} \frac{E(z)}{2(1+\nu)}bdz \tag{12}$$

The differential equations of motion can be found by substituting Eq. (10) into Eq. (8).

$$\begin{cases} Au_0'' - B\phi'' = I_0\dfrac{\partial^2 u_0}{\partial t^2} + I_1\dfrac{\partial^2 \phi}{\partial t^2} \\ k_s A_{55}(w_0'' + \phi') = I_0\dfrac{\partial^2 w_0}{\partial t^2} \\ Bu_0'' - D\phi'' - k_s A_{55}(w_0' + \phi) = I_1\dfrac{\partial^2 u_0}{\partial t^2} + I_2\dfrac{\partial^2 \phi}{\partial t^2} \end{cases} \tag{13}$$

The state space method is utilized, and the displacement components are as follows:

$$\begin{Bmatrix} u_0(x,t) \\ \phi(x,t) \\ w_0(x,t) \end{Bmatrix} = \begin{bmatrix} U(x) \\ \Phi(x) \\ W(x) \end{bmatrix} e^{i\omega t} \tag{14}$$

where ω is the eigen-frequency, substituting Eq. (14) into Eq. (13) and after some algebraic manipulations, a system of ordinary differential equations is obtained

$$\begin{cases} U'' = c_1 U + c_2 \Phi + c_3 W' \\ \Phi'' = c_4 U + c_5 \Phi + c_7 W' \\ W_0'' = c_8 \Phi' + c_9 W \end{cases} \tag{15a}$$

where the coefficientsc_i are described as:

$$\begin{gathered} c_1 = \frac{(e_{2a}e_3 - e_2e_{3a})}{C_0},\ c_2 = \frac{(e_{2a}e_4 - e_2e_{4a})}{C_0},\ c_3 = \frac{-e_2e_{5a}}{C_0}, \\ c_4 = \frac{(e_1e_{3a} - e_{1a}e_3)}{C_0},\ c_5 = \frac{(e_1e_{4a} - e_{1a}e_4)}{C_0},\ c_6 = \frac{e_1e_{5a}}{C_0}, \\ c_6 = \frac{-A_s}{A_s} = -1,\ c_8 = \frac{-I_0\omega^2}{A_s} \\ e_1 = A,\ e_2 = B,\ e_3 = -I_0\omega^2,\ e_4 = -I_1\omega^2, \\ e_{1a} = e_2, e_{2a} = D,\ e_{3a} = e_4,\ e_{4a} = (-I_2\omega^2 + A), \\ e_{5a} = A_s,\ C_0 = e_1e_{2a} - e_{1a}e_2 \end{gathered} \tag{15b}$$

The systems of Eq. (15a) can be converted into a matrix form as

$$Z'(x) = TZ(x) \tag{16}$$

where $Z(x) = \{U, U', \Phi, \Phi', W, W'\}$ is the vector of unknowns and matrix T.

$$T = \begin{bmatrix} 0 & 1 & 0 & 0 & 0 & 0 \\ c_1 & 0 & c_2 & 0 & 0 & c_3 \\ 0 & 0 & 0 & 1 & 0 & 0 \\ c_4 & 0 & c_5 & 0 & 0 & c_6 \\ 0 & 0 & 0 & 0 & 0 & 1 \\ 0 & 0 & 0 & c_7 & c_8 & 0 \end{bmatrix} \tag{17}$$

A formal solution of Eq. (16) is given by:

$$Z(x) = e^{Tx}K \tag{18}$$

K is a constant column vector derived from the boundary conditions at $x = \pm L/2$ and $e^{Tx}$is the general matrix solution of Eq. (16) which is given as:

$$e^{Tx} = [E]\begin{bmatrix} e^{\lambda_1 x} & & 0 \\ & \ddots & \\ 0 & & e^{\lambda_n x} \end{bmatrix}[E]^{-1} \tag{19}$$

where $\lambda_i (i = \overline{1,n} = \overline{1,8})$ and $[E]$ are eigenvalues and corresponding matrix of eigenvectors, respectively, associated with the matrix T.

The classical and non-classical boundary conditions are examined in this study. Non-classical boundary conditions are modeled using translational and rotational springs.

Boundary conditions can be expressed in terms of unknown function $Z(x)$ as follows:

For classical boundary conditions

$$\text{Clamped (C):}\ U = \Phi = W = 0 \tag{20a}$$

$$\text{Hinged (H):}\ U = W = BU' + D\Phi' = 0 \tag{20b}$$

$$\text{Pinned (P):}\ AU' + B\Phi' = W = BU' + D\Phi' = 0 \tag{20c}$$

$$\text{Free (F):}\ AU' + B\Phi' = BU' + D\Phi' = A_s(\Phi + W') = 0 \tag{20d}$$

And non-classical boundary conditions (E)

$$U = A_{55}(\Phi + W') \pm k_T W = BU' + D\Phi' \pm k_R \Phi = 0 \tag{21}$$

where $k_T$andk_R are the spring stiffness in translation and rotation, respectively; '+' for the left end and '-' for the right end. For simplicity, the dimensionless spring factors for translational and rotational support are defined as $\beta_T = k_T L/E_m r$ and $\beta_R = (12k_R L)/(E_m \hbar^3) r$ respectively.

A homogeneous system of equations is obtained by substituting Eq. (18) into Eqs. (20)-(21):

$$G_{ij} \rightleftarrows K_i = 0 (i, j) = \overline{1,n} = \overline{1,6} \tag{22}$$

where

$$[G(x)] = [E]\begin{bmatrix} e^{\lambda_1 x} & & 0 \\ & \ddots & \\ 0 & & e^{\lambda_n x} \end{bmatrix}[E]^{-1} \tag{23}$$

The natural frequency can be calculated by setting the determinant of G_{ij} to zero. It should be noted that a trial and error procedure need to be used to obtain the natural frequency values due to the attendant of unknown ω in matrix T.

The axial displacement is described as follows in Euler-Bernoulli beam theory:

$$u(x,t) = u_0(x,t) - z\frac{\partial w_0(x,t)}{\partial x} \tag{24}$$

Following the same steps, as the FBT, we find for CBT, the following equilibrium equations

$$\begin{cases} U'' = e_1 U + e_4 W' + e_3 W''' \\ W = e_4 U + e_5 W + e_6 W''' \end{cases} \tag{25a}$$

where the coefficientse$_i$ are described as:

$$\begin{gathered} e_1 = \frac{-I_0\omega^2}{A},\quad e_2 = \frac{-I_1\omega^2}{A},\quad e_3 = \frac{B}{A}, \\ e_4 = \frac{-(Be_1 + I_1\omega^2)}{(Be_3 - D)},\ e_5 = \frac{-I_0\omega^2}{(Be_3 - D)},\ e_6 = \frac{(I_2\omega^2 - Be_2)}{(Be_3 - D)} \end{gathered} \tag{25b}$$

For the CBT, the vector of unknowns is $Z(x) = \{U, U', W, W', W'', W'''\}$

And the matrix Tis

$$T = \begin{bmatrix} 0 & 1 & 0 & 0 & 0 & 0 \\ e_1 & 0 & 0 & e_2 & 0 & e_3 \\ 0 & 0 & 0 & 1 & 0 & 0 \\ 0 & 0 & 0 & 0 & 1 & 0 \\ 0 & 0 & 0 & 0 & 0 & 1 \\ 0 & e_4 & e_5 & 0 & e_6 & 0 \end{bmatrix} \tag{26}$$

The classical boundary conditions for CBT can be expressed in terms of unknown function $Z(x)$ as follows:

$$\text{Clamped (C):}\ U = W = W' = 0 \tag{27a}$$

$$\text{Hinged (H):}\ U = W = BU' - DW'' = 0 \tag{27b}$$

$$\text{Pinned (P):}\ AU' - BW'' = W = BU' - DW'' = 0 \tag{27c}$$

$$\begin{gathered} AU' - BW'' = BU' - DW'' \\ = BU'' - DW''' + I_1\omega^2 U - I_2\omega^2 W' = 0 \end{gathered} \tag{27d}$$

3. Continuous element method

The fundamental natural frequencies of the FGP beam with various classical and non-classical boundary conditions are investigated using a state space based approach in this section.The following material parameters are used for the FGP beam.

$E_1 = 200\text{GPa},\ \rho_1 = 7850\,\text{kg/m}^3$and $\nu = \frac{1}{3}$.

For the classical boundary conditions, the dimensionless natural frequencies is used as follows:$\bar{w}_n = \frac{w_n L^2}{\hbar}\sqrt{\frac{\rho_1}{E_1}}$

And for non-classical boundary conditions, the following expression: $\overline{\Omega}_n = \Omega_n\sqrt{\frac{\rho_1(1-\nu^2)}{E_1}}$

In Tables 1 and 2, the dimensionless natural frequencies of FGP beam is given for arbitrary boundary conditions. Various span to depth ratio (L/h) and mode are investigated. the dimensionless natural frequencies based on a state-space approach in this study is compared with those given by Noori *et al.* (2021) based on complementary functions method in the Laplace domain. It can be seen that for C-C and C-H FGP beams, the present results show well agreement with the compared results. As expected, the dimensionless natural frequencies of the C-H beam are the smallest, and those of C-C boundary conditions are the largest.

In Table 3 comprehensive numerical values of the first

Table 1 Dimensionless natural frequencies of C-C FGP beams for beam II, e_0= *0.5*

Theory	L/h	5		20		50	
	Mode	Noori, 2021	Present	Noori, 2021	Present	Noori, 2021	Present
CBT	1	6.3393	6.3393	6.4716	6.4716	6.4792	6.4793
	2	14.3789	14.3788	17.7708	17.7709	17.8492	17.8493
	3	16.5216	16.5216	34.6311	34.6312	34.9578	34.9578
	4	28.7577	28.7578	56.7868	56.7869	57.7105	57.7106
	5	30.0004	30.0005	57.5154	57.5155	86.0649	86.0652
FBT	1	5.0184	5.0184	6.3476	6.3476	6.4588	6.4589
	2	11.2715	11.2715	17.0537	17.0538	17.7262	17.7262
	3	14.3789	14.3789	32.3734	32.3735	34.5490	34.5490
	4	18.6071	18.6071	51.5379	51.5380	56.6964	56.6965
	5	26.4166	26.4167	57.5154	57.5155	83.9634	83.9637

Table 2 Dimensionless natural frequencies of C-H FGP beams for beam III, e_0= 0.5

Theory	L/h	5		20		50	
	Mode	Noori, 2021	Present	Noori, 2021	Present	Noori, 2021	Present
CBT	1	3.9919	3.9920	4.0664	4.0664	4.0706	4.0707
	2	12.1909	12.1909	13.1010	13.1010	13.1530	13.1531
	3	14.4466	14.4467	27.1685	27.1685	27.4042	27.4043
	4	23.7925	23.7925	46.0667	46.0668	46.7951	46.7953
	5	28.8252	28.8253	57.4310	57.4310	71.2861	71.2864
FBT	1	3.5386	3.5386	4.0303	4.0303	4.0648	4.0648
	2	9.6538	9.6538	12.8074	12.8074	13.1038	13.1039
	3	14.3107	14.3107	26.0699	26.0700	27.2118	27.2119
	4	17.0866	17.0866	43.2422	43.2422	46.2691	46.2692
	5	25.0473	25.0474	57.3548	57.3549	70.1226	70.1226

Table 3 First three dimensionless natural frequencies of E-E FGM beam-II, L/h=15

β	Model	e_0=0.2			e_0=0.5			e_0=0.8		
		1	2	3	1	2	3	1	2	3
10^{-2}	Lei , 2021	0.1184	0.2442	0.5176	0.123	0.2601	0.5317	0.1346	0.2893	0.5688
	Present	0.1184	0.2441	0.5169	0.1238	0.2600	0.5311	0.1346	0.2891	0.5682
10^{-1}	Lei , 2021	0.1794	0.5739	0.9883	0.1821	0.5919	1.0311	0.1918	0.6323	1.1170
	Present	0.1794	0.5738	0.9873	0.1821	0.5918	1.0303	0.1918	0.6322	1.1163
10^{0}	Lei , 2021	0.2193	0.7442	1.5228	0.2241	0.7521	1.5352	0.2381	0.7868	1.5968
	Present	0.2193	0.7442	1.5227	0.2241	0.7521	1.5351	0.2381	0.7868	1.5967
10^{1}	Lei , 2021	0.3273	0.9124	1.7671	0.3348	0.9240	1.7759	0.3549	0.9668	1.8383
	Present	0.3273	0.9124	1.7670	0.3349	0.9240	1.7758	0.3549	0.9668	1.8383
10^{2}	Lei , 2021	0.4006	1.0616	1.9843	0.4029	1.0627	1.9765	0.4190	1.0963	2.0223
	Present	0.4006	1.0616	1.9843	0.4029	1.0627	1.9765	0.4190	1.0963	2.0223
10^{3}	Lei , 2021	0.4128	1.0904	2.0315	0.4137	1.0879	2.0171	0.4286	1.1182	2.0568
	Present	0.4128	1.0904	2.0315	0.4137	1.0879	2.0171	0.4286	1.1182	2.0568
10^{8}	Lei , 2021	0.4142	1.0939	2.0374	0.4150	1.0909	2.0221	0.4297	1.1209	2.0609
	Present	0.4142	1.0940	2.0374	0.4150	1.0910	2.0221	0.4297	1.1209	2.0609
10^{13}	Lei , 2021	0.4142	1.0939	2.0374	0.4150	1.0909	2.0221	0.4297	1.1209	2.0609
	Present	0.4142	1.0940	2.0374	0.4150	1.0910	2.0221	0.4297	1.1209	2.0609

Table 4 Dimensionless natural frequencies of C-F FGP beams, e_0=0.5

Theory	Model	L/h =5			L/h =20			L/h =50		
		Beam I	Beam II	Beam III	Beam I	Beam II	Beam III	Beam I	Beam II	Beam III
CBT	1	0.9085	1.0099	0.9181	0.9151	1.0179	0.9249	0.9154	1.0184	0.9253
	2	5.4496	6.0333	5.5005	5.7180	6.3590	5.7793	5.7342	6.3788	5.7961
	3	7.0840	7.1894	7.1947	15.9366	17.7153	16.1060	16.0439	17.8461	16.2166
	4	14.328	15.7814	14.4463	28.3361	28.7578	28.7566	31.4052	34.9293	31.7428
	5	21.2520	21.5683	21.5896	31.0214	34.4614	31.3495	51.8417	57.6512	52.3973
FBT	1	0.8873	0.9819	0.8969	0.9136	1.0160	0.9235	0.9152	1.0181	0.9251
	2	4.76726	5.1638	4.8187	5.65769	6.2787	5.7189	5.7243	6.3657	5.7862
	3	7.08406	7.1894	7.1918	15.5508	17.2048	15.7193	15.9783	17.7588	16.1509
	4	11.3268	12.0905	11.4534	28.3361	28.7578	28.7542	31.1704	34.6167	31.5073
	5	18.7787	19.8181	18.9926	29.7024	32.7300	30.0300	51.2301	56.8400	51.7844

Table 5 Dimensionless frequencies of FG porous beams with elastically restrained ends, e_0= *0* , *L/h=15*

β	Beam I			Beam II			Beam III		
	1	2	3	1	2	3	1	2	3
10^{-2}	0.1184	0.2575	0.4992	0.1238	0.2600	0.5311	0.1120	0.2578	0.5061
10^{-1}	0.1666	0.5560	0.9913	0.1821	0.5918	1.0303	0.1708	0.5598	0.9959
10^{0}	0.2083	0.6900	1.4146	0.2241	0.7521	1.5351	0.2119	0.6961	1.4294
10^{1}	0.3118	0.8558	1.6438	0.3349	0.9240	1.7758	0.3146	0.8633	1.6601
10^{2}	0.3664	0.9719	1.8185	0.4029	1.0627	1.9765	0.3703	0.9822	1.8383
10^{3}	0.3745	0.9912	1.8507	0.4137	1.0879	2.0171	0.3786	1.0022	1.8715
10^{8}	0.3754	0.9935	1.8545	0.4150	1.0910	2.0221	0.3795	1.0046	1.8755
10^{16}	0.3754	0.9935	1.8545	0.4150	1.0910	2.0221	0.3795	1.0046	1.8755

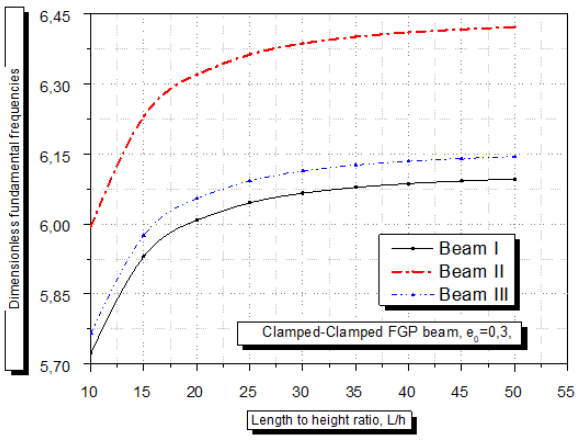

Fig. 3 Dimensionless fundamental frequencies of clamped FG porous beams as function as length-to-height ratios, $e_0 = 0.3$

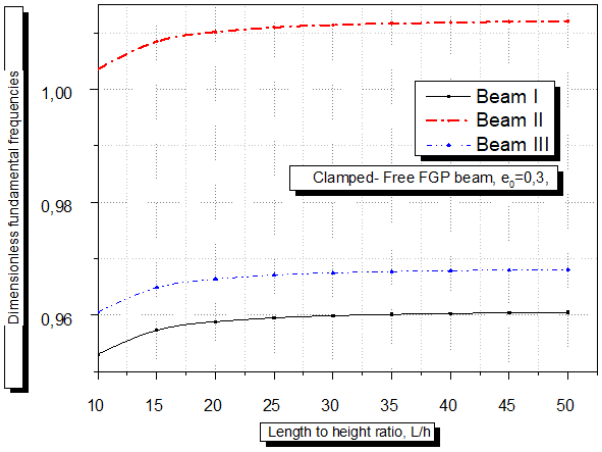

Fig. 4 Dimensionless fundamental frequencies of clamped-Free FG porous beams as function as length-to-height ratios, $e_0 = 0.3$

three dimensionless natural frequencies of E-E FGP beam-II restrained by elastic supports. The span-to-depth ratio is taken equal to L/h=15. The β parameter varies from 10-4 to 1016. It can be seen that the results are in excellent agreement with those given by Lei *et al.* (2021). Also, the dimensionless natural frequencies increase with the increase in porosity and β parameter for all first three dimensionless natural frequencies. The dimensionless natural frequencies of FGP beams with C-F and elastically restrained ends are presented in the tables 4 and 5, respectively. The volume fraction of porosity is taken equal $e_0 = 0.5$. For all case, the amplitude of vibration of the FGP beams is influenced by the variation of the distribution shape of porosity (beam I, II and III). It can conclude that the span-to-depth ratio (L/h) has a small effect on the dynamic response of FGP beams.

In Figs. 3 and 4, the dimensionless fundamental

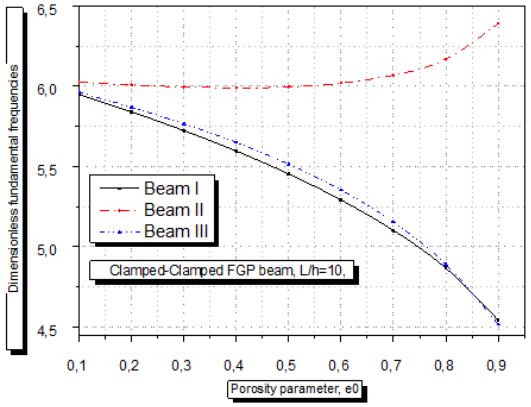

Fig. 5 Dimensionless fundamental frequencies of clamped FG porous beams, l/h=10

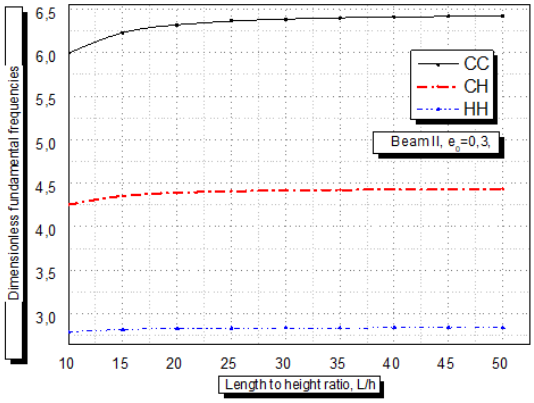

Fig. 6 Dimensionless fundamental frequencies of Beam-II with various values of length-to-height ratios, $e_0 = 0.3$

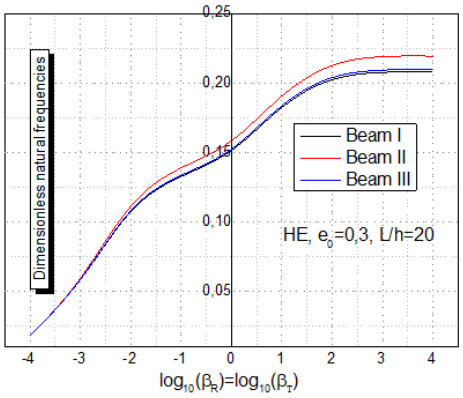

Fig. 7 Dimensionless fundamental frequencies of FG porous beams, with elastically restrained ends (HE; $e_0 = 0.3$, l/h=20)

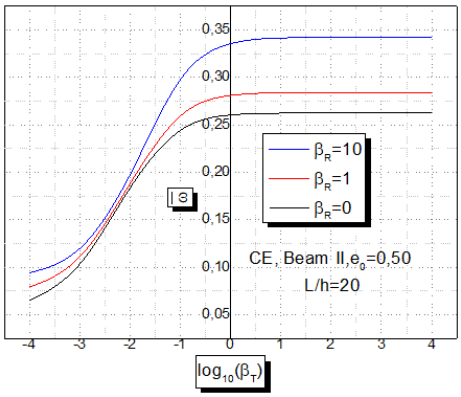

Fig. 8 Dimensionless fundamental frequencies of FG porous beam II with elastically restrained ends (CE; $e_0 = 0.3$, l/h=20)

frequencies of C-C and C-F FGP beams as function as length-to-height ratios (L/h), with varying porosity distribution shapes, respectively. The volume fraction of porosity is taken equal $e_0 = 0.3$. As shown, the length-to-height ratios is more pronounced in case of C-C FGP beam. However, the C-F FGP beam is insignificant for length-to-height ratios.

For even and uneven porosity distributions, the influence of the porosity parameter e0 on the dimensionless fundamental frequencies of clamped FGP beams is shown in Fig. 5. The length-to-height ratios is taken equal L/h=10. By increasing the porosity parameter, it is noted that, the dimensionless fundamental frequencies is increased for beam II and decreased for beam I and III sequentially. This is due to the fact that the increase of porosity parameter results in a greater reduction in the rigidity of the beam than the moment of inertia in cross-section for beams of type I and III. However, the process is reversed for type II beams.

The effect of the boundary conditions on the dimensionless fundamental frequencies of FGP beam-II as function as length-to-height ratios is shown in Fig. 6. The porosity parameter is taken equal $e_0 = 0.3$. Three types of boundary conditions are considered namely: C-C, C-H and H-H. It is noted that the dimensionless fundamental frequencies becomes more important when the boundary conditions of the FGP beam II are of type C-C.

The dimensionless fundamental frequencies of FGP beam with elastically restrained ends for different porosity distribution are presented in Figs 7 and 8. The length-to-height ratios is taken equal L/h=20. The porosity parameter is taken equal $e_0 = 0.3$and 0.5. It can be observed that with increasing of the spring constant βT in both even and uneven porosities, the dimensionless fundamental frequencies of FGP beam increases for all boundary conditions.

Fig. 9(a)-9(c) show the effect of the porosity parameter e0 on the dimensionless fundamental frequencies with varying dimensionless spring factor for three type of E-E FGP beams. The length-to-height ratios is taken equal L/h=20. the porosity parameter is taken equal to e0=0.3, 0.5 and 0.7. As can be seen from this figures, the dimensionless fundamental frequencies decreases based on the increase in the porosity parameter. The effect of the porosity parameter on the dimensionless fundamental frequencies is not noticeable when the spring constant is between $-4 \leq \beta_T \leq -2.5$.

5. Conclusions

Vibration analysis of porous functionally graded (FG) beam with classical and non-classical boundary conditions

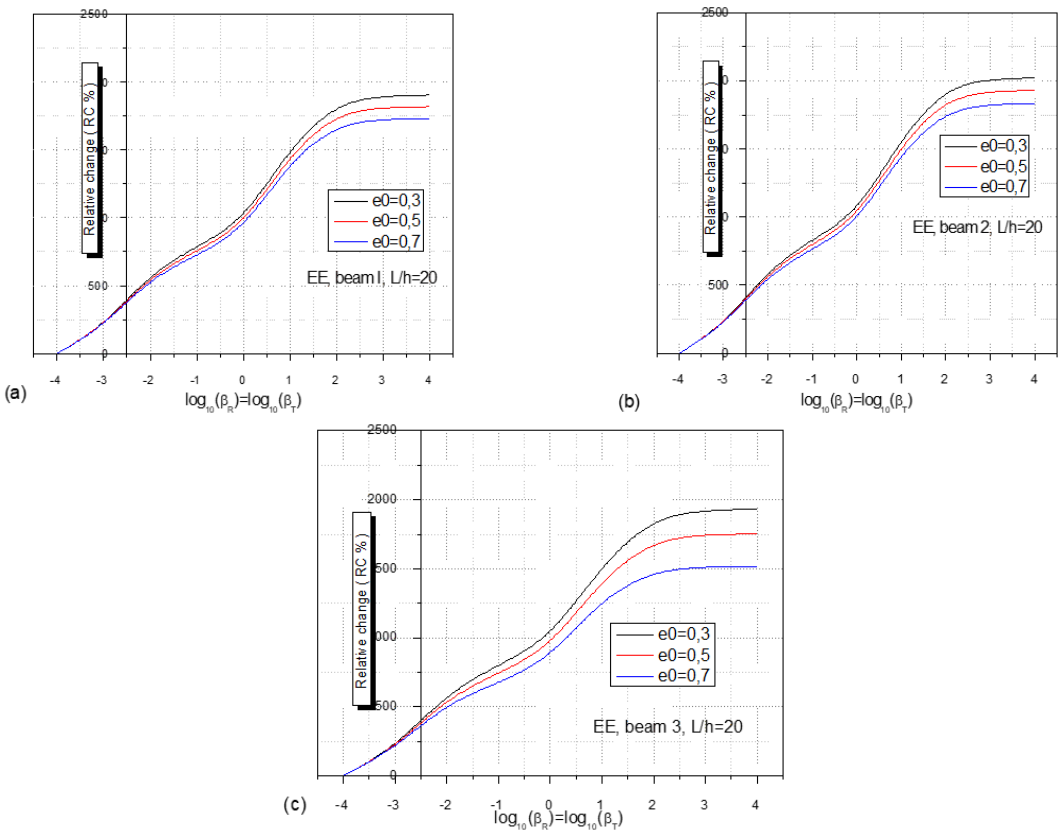

Fig. 9 Effect of e_0 on the dimensionless fundamental frequencies with varying dimensionless spring factor, l/h=20

is investigated. Three types of porosity distribution are considered as even and uneven distribution. Hamilton's principal is used to determine the equation of motion for FGP beams with various boundary conditions. The governing equation of porous FG beam is obtained using a state-space approach. The elasticity modulus of the FG beam with uneven distribution is greater than the even distribution, higher maximum dimensionless fundamental frequencies values occur at uneven distribution (beam II) for the same porosity parameter and the length-to-height ratios. The dimensionless fundamental frequencies increase based on the increase in porosity parameter in both even and uneven porosity distributions. It is seen that the porosity parameter and the length-to-height ratios is quite effective on the vibration analysis. The accuracy of the present model is justified by comparing the obtained results with those in literature. A comprehensive parametric study is presented for future works.

References

Avcar, M. (2019), "Free vibration of imperfect sigmoid and power law functionally graded beams", *Steel Compos. Struct.*, **30**(6), 603-615.http://doi.org/10.12989/scs.2019.30.6.603.

Zohra, A., Benferhat, R., Hassaine Daouadji, T. and Tounsi, A. (2021), "Analysis on the buckling of imperfect functionally graded sandwich plates using new modified power-law formulations", *Struct. Eng. Mech.*, **77**(6), 797-807. https://doi.org/10.12989/sem.2021.77.6.797.

Abdelhak, Z., Hadji, L., Hassaine Daouadji, T. and Adda Bedia, E.A. (2016), "Thermal buckling response of functionally graded sandwich plates with clamped boundary conditions", *Smart Struct. Syst.*, **18**(2), 267-291. https://doi.org/10.12989/sss.2016.18.2.267.

Abdedezak, R., Hassaine Daouadji, T., Benferhat, R. and Adim, B. (2018), "Nonlinear analysis of damaged RC beams strengthened with glass fiber reinforced polymer plate under symmetric loads", *Earthq. Struct.*, **15**(2), 113-122. https://doi.org/10.12989/eas.2018.15.2.113.

Adim, B., Hassaine Daouadji, T., Rabahi, A. and Boussad, A. (2018), "Mechanical buckling analysis of hybrid laminated composite plates under different boundary conditions", *Struct. Eng. Mech.*, **6**(6), 761-769. https://doi.org/10.12989/sem.2018.66.6.761.

Adim, B., Hassaine Daouadji, T., Rabia, B. and Hadji, L. (2016a), "An efficient and simple higher order shear deformation theory for bending analysis of composite plates under various boundary conditions", *Earthq. Struct.*, **11**(1), 63-82. https://doi.org/10.12989/eas.2016.11.1.063.

Adim, B. and Hassaine Daouadji, T. (2016b), "Effects of thickness stretching in FGM plates using a quasi-3D higher order shear deformation theory", *Adv. Mater. Res.*, **5**(4), 223-244. https://doi.org/10.12989/amr.2016.5.4.223.

Aydogdu, M. and Taskin, V. (2007), "Free vibration analysis of functionally graded beams simply supported edges", *Mater. Des.*, **28**, 1651-1656. https://doi.org/10.1016/j.matdes.2006.02.007.

Akhavan, A., Mohammadimehr, M. and Ejtahed, S. (2021), "Vibration analysis and control of porous beam integrated with FG-CNT distributed piezoelectric sensor and actuator", *Steel Compos. Struct.*, **41**(4), 595-608.

https://doi.org/10.12989/scs.2021.41.4.595.

Ammar, B., Bensattalah, T., Zidour, M. and Adda Bedia E.A. (2020), "Buckling of carbon nanotube reinforced composite plates supported by Kerr foundation using Hamilton's energy principle", *Steel Compos. Struct.*, **73**(2), 209-223. https://doi.org/10.12989/sem.2020.9.73.209.

Bian, PL. and Qing, H. (2022), "Structural analysis of nonlocal nanobeam via FEM using equivalent nonlocal differential model", *EngComput.* 1-17. https://doi.org/10.1007/s00366-021-01575-5.

Benhenni, M., Abbès, B., Hassaine Daouadji, T. and Adim, B. (2021), "Numerical modeling of hygrothermal effect on the dynamic behavior of hybrid composite plates", *Steel Compos. Struct.*, **39**(6), 751-763. http://doi.org/10.12989/scs.2021.39.6.751.

Benhenni, M., Hassaine Daouadji, T., Abbes, B., Adim, B., Yuming, L. and Abbes, F. (2018), "Dynamic analysis for anti-symmetric cross-ply and angle-ply laminates for simply supported thick hybrid rectangular plates"*Adv. Mater. Res.*, **7**(2), 83-103. https://doi.org/10.12989/amr.2018.7.2.119.

Benhenni, M., Hassaine Daouadji, T., Abbes, B., Abbes, F. and Adim, B. (2019), "Numerical analysis for free vibration of hybrid laminated composite plates for different boundary conditions", *Steel Compos. Struct.*, **70**(5), 535-549. https://doi.org/10.12989/sem.2019.70.5.535.

Bensattalah, T. and Hassaine Daouadji, T. (2020), "Improved analytical solution for slip and interfacial stress in composite steel-concrete beam bonded with an adhesive", *Adv. Mater. Res.*, **9**(2),133-153.https://doi.org/10.12989/amr.2020.9.2.133.

Bensattalah, T., Zidour, M. and Hassaine Daouadji, T. (2018), "Analytical analysis for the forced vibration of CNT surrounding elastic medium including thermal effect using nonlocal Euler-Bernoulli theory", *Adv. Mater. Res.*, **7**(3), 163-174. https://doi.org/10.12989/amr.2018.7.3.163.

Bensattalah, T., Zidour, M. and Hassaine Daouadji, T. (2019), "A new nonlocal beam model for free vibration analysis of chiral single-walled carbon nanotubes", *Compos. Mater. Eng.*, **1**(1), 21-31. http://dx.doi.org/10.12989/cme.2019.1.1.021.

Bensatallah, T., Hassaine Daouadji, T., Rabahi, A. and Tounsi, A. (2021), "Structural bonding for civil engineering structures: New model of composite I-steel-concrete beam strengthened with CFRP plate", *Steel Compos. Struct.*, **41**(3), 417-435. https://doi.org/10.12989/scs.2021.41.3.417.

Rabia, B., Abderezak, R., Hassaine Daouadji, T., Abbes, B., Belkacem, A. and Abbes, F. (2018), "Analytical analysis of the interfacial shear stress in RC beams strengthened with prestressed exponentially-varying properties plate", *Adv. Mater. Res.*, **7**(1), 29-44. https://doi.org/10.12989/amr.2018.7.1.029.

Rabia, B., Hassaine Daouadji, T. and Abderezak, R. (2019), "Effect of distribution shape of the porosity on the interfacial stresses of the FGM beam strengthened with FRP plate", *Earthq. Struct.*, **16**(5), 601-609. https://doi.org/10.12989/eas.2019.16.5.601.

Benferhat, R., Hassaine Daouadji, T. and Abderezak, R. (2021), "Effect of porosity on fundamental frequencies of FGM sandwich plates", *Compos. Mater. Eng.*, **3**(1), 25-40. http://doi.org/10.12989/cme.2021.3.1.025.

Benferhat, R., Hassaine Daouadji, T. and Rabahi, A. (2021a), "Effect of porosity on fundamental frequencies of FGM sandwich plates", *Compos. Mater. Eng.*, **3**(1), 25-40. http://doi.org/10.12989/cme.2021.3.1.025.

Benferhat, R., Hassaine Daouadji, T. andRabahi, A.(2021b), "Effect of air bubbles in concrete on the mechanical behavior of RC beams strengthened in flexion by externally bonded FRP plates under uniformly distributed loading", *Compos. Mater. Eng.*, **3**(1), 41-55. http://dx.doi.org/ 10.12989/cme.2021.3.1.041.

Benferhat, R., Hassaine Daouadji, T. and Rabahi, A. (2021c), "Analysis and sizing of RC beams reinforced by external bonding of imperfect functionally graded plate", *Adv. Mater. Res.*, **10**(2), 77-98. http://doi.org/10.12989/amr.2021.10.2.077.

Bourada, F., Bousahla, A.A., Bourada, M., Azzaz, A., Zinata, A. and Tounsi, A. (2019), "Dynamic investigation of porous functionally graded beam using a sinusoidal shear deformation theory", *Wind Struct.*, **28**(1), 19-30. https://doi.org/10.12989/was.2019.28.1.019.

Berghouti, H., Adda Bedia, E.A., Benkhedda, A. and Tounsi, A. (2019), "Vibration analysis of nonlocal porous nanobeams of functionally graded material", *Adv. Nano Res.*, **7**(5), 351-364. https://doi.org/10.12989/anr.2019.7.5.351.

Hadj, B., Rabia, B. and Daouadji, T.H. (2019), "Influence of the distribution shape of porosity on the bending FGM new plate model resting on elastic foundations", *Struct. Eng. Mech.*, **72**(1), 823-832. https://doi.org/10.12989/sem.2019.72.1.061.

Hadj, B., Rabia, B. and Hassaine Daouadji, T. (2021), "Vibration analysis of porous FGM plate resting on elastic foundations: Effect of the distribution shape of porosity", *Coupled Syst. Mech.*, **10**(1),61-77. http://doi.org/10.12989/csm.2021.10.1.061.

Chergui, S., Hassaine Daouadji, T., Mostefa, H., Bougara, A., Abbes, B. and Amziane, S. (2019), "Interfacial stresses in damaged RC beams strengthened by externally bonded prestressed GFRP laminate plate: Analytical and numerical study", *Adv. Mater. Res.*, **8**(3),197-217. https://doi.org/10.12989/amr.2019.8.3.197.

Chaded, A., Hassaine Daouadji, T., Rabahi, A., Adim, B., Benferhat, R. and Fazilay, A. (2018), "A high-order closed-form solution for interfacial stresses in externally sandwich FGM plated RC beams", *Adv. Mater. Res.*, **6**(4), 317-328. https://doi.org/10.12989/amr.2017.6.4.317.

Civalek, O. and U. Busra (2020), "Frequency, bending and buckling loads of nanobeams with cross sections", *Adv. Nano Res.*,**9**(2), 91-104. https://doi.org/10.12989/anr.2020.9.2.091.

Dehshahri, K., Nejad, M.Z., Ziaee, S., Niknejad, A. and Hadi, A. (2020), "Free vibrations analysis of arbitrary three-dimensionally FGM nanoplates", *Adv. Nano Res.*, **8**(2), 115-134. https://doi.org/10.12989/anr.2020.8.2.115.

Demir, E., Çallıoğlu, H., Sayer, M. andKavla, F. (2020), "Effect of chitosan/carbon nanotube fillers on vibration behaviors of drilled composite plates", *Steel Compos. Struct.*, **35**(6), 789-798. https://doi.org/10.12989/scs.2020.35.6.789.

Ebrahimi, F., Barati, M.R. and Civalek, Ö. (2019), "Application of Chebyshev–Ritz method for static and vibration analysis of nonlocal microstructure-dependent nanostructures", *Eng. Comput.*, **36**, 953-964. https://doi.org/10.1007/s00366-0190742.

Ebrahimi, F., Karimiasl, M. and Mahesh, V. (2021), "Chaotic dynamics and forced harmonic vibration analysis of magneto-electro-viscoelastic multiscale composite nanobeam", *Eng. Comput.*, **37**, 937-950. https://doi.org/10.1007/s00366-019-00865-3.

Ebrahimi, F. and Hosseini, S.H.S. (2020), "Effect of residual surface stress on parametrically excited nonlinear dynamics and instability of double-walled nanobeams: an analytical study", *Eng. Comput.*, **37**, 1219-1230. https://doi.org/10.1007/s00366-019-00879-x.

Fakher, M. and Hosseini-Hashemi, S. (2022), "Vibration of two-phase local/nonlocal Timoshenko nanobeams with an efficient shear-locking-free finite-element model and exact solution", *Eng. Comput.*, **38**, 231-245. https://doi.org/ 10.1007/s00366-020-01058-z.

Ebrahimi, F., Hosseini, S.H.S. and Selvamani, R. (2020), "Thermo-electro-elastic nonlinear stability analysis of viscoelastic double-piezo nanoplates under magnetic field", *Struct. Eng. Mech.*,**73**(5), 565-584. https://doi.org/10.12989/sem.2020.73.5.565.

She, G.L., Liu, H.B. andKarami, B. (2020), "On resonance behavior of porous FG curved nanobeams", *Steel Compos. Struct*,**36**(2), 179-186. https://doi.org/10.12989/scs.2020.36.2.179.

She, G.L. (2020), "Wave propagation of FG polymer composite nanoplates reinforced with GNPs", *Steel Compos. Struct*.,**37**(1), 27-35. https://doi.org/10.12989/scs.2020.37.1.027.

Hamrat, M., Bouziadi, F., Bensaid, B., Hassaine Daouadji, T., Chergui, S., Labed, A. and Amziane, S. (2020), "Experimental and numerical investigation on the deflection behavior of pre-cracked and repaired reinforced concrete beams with fiber-reinforced polymer", *Construct. Build. Mater*., **249**,1-13. http://doi.org/10.1016/j.conbuildmat.2020.118745.

Hassaine Daouadji, T. (2017), "Analytical and numerical modeling of interfacial stresses in beams bonded with a thin plate", *Adv. Comput. Des*., **2**(1), 57-69. https://doi.org/10.12989/acd.2017.2.1.057.

Hassaine Daouadji, T., Bensattalah, T., Rabahi, A. and Tounsi, A. (2021a), "New approach of composite wooden beam- reinforced concrete slab strengthened by external bonding of prestressed composite plate: Analysis and modeling", *Struct. Eng. Mech*. **78**(3), 319-332. http://doi.org/10.12989/sem.2021.78.3.31.

Hassaine Daouadji, T., Rabahi, A., Benferhat, R. and Tounsi, A. (2021b), "Performance of damaged RC continuous beams strengthened by prestressed laminates plate: Impact of mechanical and thermal properties on interfacial stresses", *Coupled Syst. Mech*., **10**(2), 161-184. http://doi.org/10.12989/csm.2021.10.2.161.

Hassaine Daouadji, T., Rabahi, A., Benferhat, R., and Tounsi, A. (2021c), "Impact of thermal effects in FRP-RC hybrid cantilever beams", *Struct. Eng. Mech*.,**78**(5), 573-583. http://doi.org/10.12989/sem.2021.78.5.573.

Hassaine Daouadji, T., Rabahi, A. and Benferhat, R. (2021d), "A new model for adhesive shear stress in damaged RC cantilever beam strengthened by composite taking into account the effect of creep shrinkage", *Struct. Eng. Mech*., **79**(5), 531-540. http://doi.org/10.12989/sem.2021.79.5.531.

Hassaine Daouadji, T., Rabahi, A. and Benferhat, R. (2021e), "Hyperstatic steel structure strengthened with prestressed carbon/glass hybrid laminated plate", *Coupled Syst. Mech*., **10**(5), 393-414. https://doi.org/10.12989/csm.2021.10.5.393.

Kablia, A., Benferhat, R., Hassaine Daouadji, T. and Bouzidene, A. (2020), "Effect of porosity distribution rate for bending analysis of imperfect FGM plates resting on Winkler-Pasternak foundations under various boundary conditions", *Coupled Syst. Mech*., **9**(6), 575-597. http://doi.org/10.12989/csm.2020.9.6.575.

Karama, M., Afaq K.S. and Mistou, S. (2003), "Mechanical behavior of laminated composite beam by the new multi-layered laminated composite structures model with transverse shear stress continuity", *Int. J. Solids Struct*.,**40**(5), 25-46. http://doi.org/10.1016/S0020-7683(02)00647-9.

Lei, Y.L., Kang, G., Xinwei, W. and Jie, Y. (2020), "Dynamic behaviors of single- and multi-span functionally graded porous beams with flexible boundary constraints", *Appl. Math. Modell*., **83**, 754-776. https://doi.org/10.1016/j.apm.2020.03.017.

Mahsa, N. and Isa, A. (2021), "A nonlocal Layerwise theory for free vibration analysis of nanobeams with various boundary conditions on Winkler-Pasternak foundation", *Steel Compos. Struct*., **40**(1), 101-119. https://doi.org/10.12989/scs.2021.40.1.101.

Mohsen, M. and Arameh, E. (2020), "Post-buckling analysis of Mindlin Cut out-plate reinforced by FG-CNTs", *Steel Compos. Struct*, **34**(2), 289-297. https://doi.org/10.12989/scs.2020.34.2.289.

Mohammad, A. and Kamil Żur, K. (2020), "Free vibration analysis of functionally graded nanoshells resting on Pasternak foundation based on two-dimensional analysis", *Steel Compos. Struct*, **34**(4), 615-623. https://doi.org/10.12989/scs.2020.34.4.615.

Nazemnezhad, R., Rabiei, M. and Pouyan, S. (2021), "Large amplitude free torsional vibration analysis of size-dependent circular nanobars using elliptic functions", *Struct. Eng. Mech*.,**77**(4), 535-547. https://doi.org/10.12989/sem.2021.77.4.535.

Noroozi, R., Kazemi, A., Norouzi, S. and Hadi, A. (2020), "Torsional vibration analysis of bi-directional FG nano-cone with arbitrary cross-section based on nonlocal strain gradient elasticity", *Adv. Nano Res*., **8**(1), 13-24. https://doi.org/10.12989/anr.2020.8.1.013.

Noori, A.R., Timuçin, A.A. and Beytullah, T. (2021), "Dynamic analysis of functionally graded porous beams using complementary functions method in the laplace domain", *Compos. Struct*.,**256**, 113094. https://doi.org/10.1016/j.compstruct.2020.113094.

Ran, B., Gao, J., and Seyedmahmoodreza, A. (2021), "Higher order plate theory for buckling analysis of plates based on exact solution", *Steel Compos. Struct*.,**40**(3), 451-459. https://doi.org/10.12989/scs.2021.40.3.451.

Reza, N. and Shokrollahi, H. (2020), "Free axial vibration of cracked axially functionally graded nanoscale rods incorporating surface effect", *Steel Compos. Struct*, **35**(3), 449-462. https://doi.org/10.12989/scs.2020.35.3.449.

Rabahi, A., Hassaine Daouadji, T. and Benferhat, R. (2021a), "Modeling and analysis of the imperfect FGM-damaged RC hybrid beams", *Adv. Comput. Des*., **6**(2), 117-133. http://doi.org/10.12989/acd.2021.6.2.117.

Rabahi, A., Hassaine Daouadji, T. and Benferhat, R.(2021b), "Aluminum beam reinforced by externally bonded composite materials", *Adv. Mater. Res*., **10**(1), 23-44. http://doi.org/10.12989/amr.2021.10.1.023.

Rabahi, A., Hassaine Daouadji, T., Benferhat, R. and Tounsi, A. (2021c), "Mechanical behavior of RC cantilever beams strengthened with FRP laminate plate", *Adv. Comput. Des*., **6**(3), 169-190. http://doi.org/10.12989/acd.2021.6.3.169.

Rabahi, A., Hassaine Daouadji, T., Benferhat. R. and Tounsi, A. (2021d), "New proposal for flexural strengthening of a continuous I-steel beam using FRP laminate under thermo-mechanical loading", *Struct. Eng. Mech*.,**78**(6), 703-714. http://doi.org/10.12989/sem.2021.78.6.703.

Rabahi, A., Hassaine Daouadji, T. and Benferhat, R. (2021e), "Fiber reinforced polymer in civil engineering: Shear lag effect on damaged RC cantilever beams bonded by prestressed plate", *Coupled Syst. Mech*.,**10**, 299-316. http://doi.org/10.12989/csm.2021.10.4.299.

Rabahi, A., Hassaine Daouadji, T. and Benferhat, R. (2021f), "New solution for damaged porous RC cantilever beams-strengthening by composite plate", *Adv. Mater. Res*., **10**(3), 169-194. http://doi.org/10.12989/amr.2021.10.3.169.

Reddy, J.N. (1984), "A simple higher-order theory for laminated composite plates", *J. Appl. Mech*., **51**(4), 745-752. https://doi.org/10.1115/1.3167719.

Simsek, M. (2009), "Fundamental frequency analysis of functionally graded beams by using different higher-order beam theories", *Nuclear Eng. Des*., **240**(4), 697-705. http://doi.org/10.1016/j.nucengdes.2009.12.013.

Shanab, R.A. and Attia, M.A. (2020), "Semi-analytical solutions for static and dynamic responses of bi-directional FG nonuniform nanobeams with surface energy effect", *Eng. Comput*., 1-44. https://doi.org/10.1007/s00366-020-01205-6.

Sayyid, H. and Hashemi, K. (2020), "Nonlinear and nonclassical vibration analysis of double walled piezoelectric cylindrical nanoshell", *Adv. Nano Res*., **9**(4), 277-294. https://doi.org/10.12989/anr.2020.9.4.277.

Singh Piyush, P. and Azam, M.S. (2021), "Size dependent vibration of functionally graded nanoplate in hygrothermal environment by Rayleigh-Ritz method", *Adv*. *Nano Res*., **10**(1), 25-42. https://doi.org/10.12989/anr.2021.10.1.025.

Tlidji, Y., Benferhat, R. and Hassaine Daouadji, T. (2021a), "Study and analysis of the free vibration for FGM microbeam containing various distribution shape of porosity", *Struct*. *Eng*. *Mech*.,**77**(2), 217-229. http://doi.org/10.12989/sem.2021.77.2.217.

Tlidji, Y., Benferhat, R., Luan C.T., Hassaine Daouadji, T. and Tounsi, A. (2021b), "New state-space approach to dynamic analysis of porous FG beam under different boundary conditions", *Adv*. *Nano Res*., **11**(4), 347-359. https://doi.org/10.12989/.2021.11.4.347.

Tounsi, A., Al-Dulaijan, S.U., Al-Osta, A., Abdelbaki, C., Alzahrani, M.M. and Alfarabi, S. (2020), "A four variable trigonometric integral plate theory for hygro-thermo-mechanical bending analysis of AFG ceramic-metal plates resting on a two-parameter elastic foundation", *Steel Compos*. *Struct*., **34**(4), 511-524. https://doi.org/10.12989/scs.2020.34.4.511.

Wattanasakulpong, N. and Ungbhakorn, V. (2012), "Free vibration analysis of functionally graded beams with general elastically end constraints by DTM", *World J*. *Mech*., **2**(6), 297-312. http://doi.org/10.4236/wjm.2012.26036.

Wattanasakulpong, N. and Ungbhakorn, V. (2014), "Linear and nonlinear vibration analysis elastically restrained FGM beams with porosities", *Aerosp*. *Sci*. *Technol*.,**32**(1), 111-120, http://doi.org/10.1016/j.ast.2013.12.002.

Xinli, X., Chunwei, Z., Farayi, M., Tamer, A.S. and Afrasyab, K. (2021), "Dispersion of waves characteristics of laminated composite nanoplate", *Steel Compos*. *Struct*., **40**(3), 355-367. https://doi.org/10.12989/scs.2021.40.3.355.

Yaser, S.F., Mohamadreza, S. and Seyed, M., Mosavi, N. (2020), "Meshless Local Petrov-Galerkin (MLPG) method for dynamic analysis of non-symmetric nanocomposite cylindrical shell", *Struct*. *Eng*. *Mech*., **74**(5), 679-698. https://doi.org/10.12989/sem.2020.74.5.679.

Zaoui, F.Z., Younsi, A., Meradjah, M., Tounsi A. and Ouinas, D. (2017), "Free vibration analysis of functionally graded beams using a higher-order shear deformation theory", *Math*. *Model*. *Eng*. *Probl*., **4**(1), 7-12. https://doi.org/10.18280/mmep.040102.

JL